

Enhancing Black-Litterman Portfolio via Hybrid Forecasting Model Combining Multivariate Decomposition and Noise Reduction

Ziye Yang, Ke Lu

Abstract—The sensitivity to input parameters and lack of flexibility limits the traditional Mean-Variance model. In contrast, the Black-Litterman model has attracted widespread attention by integrating market equilibrium returns with investors' subjective views. This paper proposes a novel hybrid deep learning model combining Singular Spectrum analysis (SSA), Multivariate Aligned Empirical Mode Decomposition (MA-EMD), and Temporal Convolutional Networks (TCNs), aiming to improve the prediction accuracy of asset prices and thus enhance the ability of the Black-Litterman model to generate subjective views. Experimental results show that noise reduction pre-processing can improve the model's accuracy, and the prediction performance of the proposed model is significantly better than that of three multivariate decomposition benchmark models. We construct an investment portfolio by using 20 representative stocks from the NASDAQ 100 index. By combining the hybrid forecasting model with the Black-Litterman model, the generated investment portfolio exhibits better returns and risk control capabilities than the Mean-Variance, Equal-Weighted, and Market-Weighted models in the short holding period.

Index Terms—Black-Litterman model, Portfolio optimization, Stock prediction, Multivariate decomposition, Hybrid model, Deep learning

I. INTRODUCTION

IN 1952, Harry Markowitz introduced Modern Portfolio Theory (MPT) to revolutionize portfolio management by optimizing the risk-return balance through mean-variance analysis [1]. However, MPT faces many challenges in practical applications. Its extreme sensitivity to input parameters often leads to large changes in asset weights [2], and traditional mean-variance optimizers amplify estimation errors and ignore input uncertainty [3]. Faced with the limitations of MPT, the researchers did not stop there. In 1992, Fisher Black and Robert Litterman proposed the Black-Litterman (BL) model [4]. The model is based on Bayesian statistics and combines CAPM market equilibrium information with investors' subjective views to generate a new posterior distribution of returns and optimize portfolio construction for more scientific and rational asset allocation [5]–[7]. Bessler and Wolff [8] show that portfolios based on this model have higher net Sharpe ratios, lower risk and better diversification out of sample.

Despite the advantages of BL models in incorporating investors' subjective insights, how to accurately predict asset movements to obtain subjective insights with high accuracy is still the focus of extensive discussions among scholars. In our review of the relevant literature, we found that most of these studies use different forecasting models to analyze historical

data and predict future price fluctuations to obtain an investor's view with a high degree of accuracy. These approaches include traditional econometric models [9]–[11], as well as hybrid models combining econometrics and machine learning [12], [13].

Decomposition Ensemble models (DEMs) emerged with the development of signal decomposition and deep learning, providing a breakthrough for financial market forecasting. DEM decomposes the original sequence into multiple intrinsic mode functions (IMFs) by introducing the Empirical Mode decomposition (EMD) [14] and then integrates the results after predicting different frequency components. Experiments have shown that DEMs are significantly better than traditional models in predictive performance [15]–[17] and have been applied to the study of opinion generation [18], [19].

However, when predicting financial data, multiple variables can better explain stock price trends than single variables and scholars have proposed various multivariate prediction model [20], [21]. The above DEM methods are based on decomposing closing prices (single variable). The EMD algorithm cannot guarantee the consistency of the number of IMFs obtained from the decomposition of each signal. Therefore, scholars focus on Multivariate Empirical Mode Decomposition (MEMD) [22], which can jointly decompose multidimensional signals to ensure that the IMFs of each dimensional signal match in quantity and frequency scale. Recently, MEMD-based multivariate decomposition ensemble models (M-DEMs) have been widely used in financial markets, and their prediction accuracy is better than that of traditional single-variable DEMs [23]–[26]. Among them, Yao et al. [26] proposed the MEMD-TCN hybrid model for stock index prediction, and they emphasized that the TCNs take less memory in training, have higher accuracy, and avoid the problem of gradient explosion or gradient vanishing, which is common in RNNs.

Research into multivariate decomposition algorithms continues, with a subset of articles pointing out that MEMD requires long computation times when dealing with high-dimensional data [27], [28]. In addition to the inefficiency, Cai et al. [29] experimentally demonstrated that the decomposition quality of MEMD is far inferior to that of EMD by using periodicity and symmetry metrics. This defect affects the subsequent prediction accuracy. They propose a new algorithm for the prediction task, Multivariate Aligned Empirical Mode Decomposition (MA-EMD). Based on EMD, the algorithm measures the difference between IMFs based on the frequency representation of the extreme points, thus realizing the alignment of IMFs. So far, no scholars have applied the MA-EMD algorithm to forecast the movement of financial assets.

Ziye Yang is with the Institute of Collaborative Innovation, University of Macau 999078, China (e-mail: mc46468@um.edu.mo).

Ke Lu is with the Faculty of Technology, University of Macau 999078, China (e-mail: yc37949@um.edu.mo).

Another issue that cannot be ignored is how to reduce the impact of noise in financial data on predictions. These noises may originate from random market transaction fluctuations, interference from external factors and so on [30]. Many studies have shown that the accuracy of financial time series forecasting tasks can be effectively enhanced by appropriate noise reduction methods [31]–[34], but most decomposition-ensemble models do not consider the noise problem [35]. As a result, the model may overfit the noisy data during the training process, the prediction may be biased, or underfitting may occur when it is difficult to capture the valid information in the data accurately [36].

To address the problems of existing studies, this paper proposes a new SSA-MAEMD-TCN model based on the "M-DEM" forecasting framework, aiming to improve the forecasting accuracy of asset prices and thus enhance the ability to generate investor perspectives in the Black-Litterman model. The characteristics of this hybrid model are: 1) using MAEMD instead of MEMD to achieve more efficient sequence decomposition; 2) introducing the singular spectrum analysis (SSA) method [37], which is very effective in financial data [38]–[40], for noise reduction; 3) using TCNs instead of RNNs to predict the IMFs component. The U.S. stock data from January 2020 to September 2023 is selected as the experimental target, aiming to test the proposed model's predictive performance and portfolio performance. We document the difference in predictive metrics between SSA-MAEMD-TCN and the benchmark model and compare the performance of Black-Litterman based on the predictive model with the rest of the portfolio models in terms of return, volatility, and other performance over different holding periods.

The contributions include the following points: 1) Explore the application of the MA-EMD algorithm in financial time series forecasting, confirm its advantages in processing financial data, and provide a reference for subsequent research. 2) Propose an SSA-MAEMD-TCN hybrid model to reduce the impact of noise, achieve efficient series decomposition, and improve forecasting performance. 3) The hybrid model provides more accurate investor views for the Black-Litterman model, optimizing portfolio construction.

The structure of this paper is as follows: Section II reviews some methods for generating subjective opinions and the application of M-DEMs and SSA in financial markets. Section III explores the theoretical basis of core technologies. Section IV introduces the overall experimental framework and steps. Section V evaluates the experimental results, focusing on prediction accuracy and portfolio performance. Section VI summarizes the main findings and discusses future research directions.

II. RELATED WORK

This research focuses on the academic areas of generating investor perspectives to enhance BL portfolio and applying M-DEMs and SSA method in financial market.

Early studies mainly generated subjective views through traditional econometric models. Beach and Orlov [9] first applied the EGARCH-M model to global asset allocation,

dynamically estimated the expected returns and conditional variances of assets in 20 countries, and generated dynamic opinions for the BL model, with returns exceeding the market equilibrium weight and Markowitz optimal allocation. Palomba [10] combined the multivariate GARCH model with the BL model and used the FDCC model to estimate and predict asset returns and covariance matrices, achieving better risk-return balance and higher information ratio in tactical asset allocation (TAA). Duqi et al. [11] used the EGARCH-M model to capture volatility clustering, leverage effects, and asymmetry, construct stock portfolios at different risk levels, and calculate expected excess returns through the BL model, performing well in risk-stratified allocation.

As machine learning advances, blending econometric and machine learning models effectively generates investor views in BL models. Pyo and Lee [12] combined three machine learning models (Gaussian Process Regression, Support Vector Regression, and Artificial Neural Networks) with the GARCH model to forecast asset volatility in the KS200. They divided assets into high-risk and low-risk groups, constructing a BL portfolio reflecting investor views. Results showed this portfolio had higher Sharpe ratios and positive alpha. Kara et al. [13] used the GARCH model to predict stock indices and Support Vector Regression to map volatility forecasts to return forecasts, generating investor-view vectors for the BL model. This approach outperformed market indices in the BIST-30 and DJI, showing better portfolio returns and Sharpe ratios across holding periods. Lei [41] proposed a PCA-AHP framework to tackle overfitting in high-dimensional asset allocation, reducing prediction errors in Chinese stock-market sector indices via dimensionality reduction and weight optimization in the BL model.

Recently, decomposed ensemble models (DEMs) have gradually emerged. DEMs use EMD [14] and its improved methods, such as EEMD [42], CEEMD [43], and CEEMDAN [44], to provide a new approach to asset prediction tasks through the "decompose-predict-reconstruct" strategy. Rezaei et al. [18] developed a CEEMD-CNN-LSTM hybrid model for stock price prediction. Investor views based on its predictions significantly enhance asset allocation effectiveness. Barua and Sharma [45] used a CNN-BiLSTM model to predict future stock prices and a dynamic EWMA covariance matrix to emphasize recent data. Their follow-up study [19] built a CEEMDAN-GRU-XGBoost framework, using GRU to predict sentiment indicators and XGBoost to generate ETF views. The improved BL model outperformed others over six investment periods.

Most DEMs are univariate forecasting models that only decompose and forecast closing prices. Multivariate versions of EMD have been developed, including B-EMD [46], T-EMD [47], and MEMD [22]. MEMD is widely used in financial forecasting and forms Multivariate Decomposition Ensemble models (M-DEMs). Deng et al. [23] proposed the MEMD-LSTM model, combining MEMD for multidimensional time-frequency analysis and feature extraction with OATM-optimized LSTM hyperparameters. Experiments show that its multistep prediction surpasses EMD-LSTM and traditional LSTM. Zou and He [24] developed a MEMD-CNN

multiscale model for risk prediction, outperforming single-scale models like ARMA-GARCH and VMD-CNN. Bai et al. [25] built a hybrid prediction model blending "fuzzy computing" and "decomposition-ensemble". Using MPE for feature selection, MI and NRS for filtering, and MEMD for decomposition, features entered an LSTM network. Though capturing market complexity, it struggles with unexpected events and has prediction delays. Yao et al. [26] proposed a hybrid MEMD-TCN model for stock index prediction, decomposing multidimensional data like opening, high, low, closing prices and trading volumes. The model outperforms univariate DEM and M-DEM combined with recurrent neural networks (RNNs) in stock index forecasting in several countries. It also emphasizes the superiority of TCNs compared to rnns.

However, MEMD suffers from computational inefficiency when dealing with multivariate data. Lang et al. [27] proposed the FMEMD algorithm, which is far more computationally efficient than MEMD when dealing with large-scale multidimensional signals. s. Thirumalaisamy and Ansell [48] proposed the FAMVEMD algorithm, which is much more practical when dealing with one-dimensional and three-dimensional synthetic signals. In addition to being computationally slow, Cai et al. [29], standing for the prediction task, also pointed out that MEMD suffers from relaxing the quality constraints on subsequences, generating unnecessary frequency components, which negatively affects the final prediction performance. For this reason, they proposed Multivariate Aligned Empirical Mode Decomposition (MA-EMD). The algorithm first applies the standard EMD to each variable individually and then takes the IMFs of the target variable as a reference, uses the Kullback-Leibler dispersion (KLD) to measure the frequency similarity between the IMFs of different variables and aligns them to the corresponding sub-prediction models. It is experimentally demonstrated that M-DEM combined with MA-EMD outperforms the MEMD-based model regarding prediction accuracy.

In addition, reducing noise in financial data is another effective strategy to improve prediction results. However, existing DEM and M-DEM frameworks seldom consider the effects of noise when predicting financial data [35]. Singular Spectrum Analysis (SSA) [37] is a powerful noise reduction algorithm that is very effective in financial forecasting tasks. Lahmiri [38] proposed an intraday stock price prediction method based on SSA and Support Vector Regression (SVR) combined with Particle Swarm Optimization (PSO). Experimental results show that the method outperforms traditional prediction models in terms of accuracy. Tang et al. [39] used wavelet transform (WT) and SSA to reduce the raw data and then input the smoothed sequences into LSTM for prediction. This approach resulted in better prediction performance than feeding the original sequences directly into LSTM. [40] proposed a hybrid deep learning framework SSA-PSO-LSTM for predicting stock index prices and their fluctuations. Experimental results show that this method has higher prediction accuracy during high volatility than the remaining models, such as PSO-LSTM.

In summary, existing research has achieved some results in generating investor views and applying M-DEM, but there is

still room for improvement. This paper proposes a hybrid SSA-MAEMD-TCN stock price prediction model, which provides a new method for generating investor opinions and fills the research gap of M-DEMs in this field.

III. TECHNICAL BACKGROUND

A. Black-Litterman Model

To solve the problems of input sensitivity and estimation error maximization in traditional mean-variance optimization, Fischer Black and Robert Litterman developed the Black-Litterman model. Fig. 1 illustrates the key parameters and process of the Black-Litterman model, and the specific steps are as follows:

1) *Calculating Priori Returns*: Starting from market equilibrium conditions, prior estimates of asset expected returns are derived through reverse optimization. Specifically, assuming that the market portfolio weights are based on market capitalization, the implied equilibrium returns are obtained using the reverse process of mean-variance optimization, as shown below:

$$\Pi = \lambda \Sigma w_{mkt} \quad (1)$$

where, Π is the implied excess return vector ($N \times 1$), λ is the risk aversion parameter. In this paper, we set $\lambda = 2.5$ to represent the world average risk aversion index. Σ is the covariance matrix of excess returns ($N \times N$), w_{mkt} is the vector of asset weights based on market capitalization ($N \times 1$).

2) *Setting Investor Views*: Investor views are treated as new information, and the distribution of these views is calculated. Investor views can be absolute (e.g., the expected return of a specific asset is 5%) or relative (e.g., the expected return of one asset is higher than another). The investor's views are converted into the following three parameters:

View Matrix P : The view matrix P is a $k \times n$ matrix, where k is the number of views and n is the number of assets. It maps the investor's views onto specific assets, indicating which assets correspond to each view. Since we are only considering absolute views, each row of the P matrix will have exactly one non-zero element, which is located in the column corresponding to the asset and equals 1. Specifically, suppose you have k absolute views, corresponding to assets i_1, i_2, \dots, i_k (where i_j is the index of the asset, and $1 \leq i_j \leq n$), then the matrix P can be represented as:

$$P = \begin{bmatrix} 0 & 0 & \dots & 1 & \dots & 0 \\ 0 & 0 & \dots & 1 & \dots & 0 \\ \vdots & \vdots & \ddots & \vdots & \ddots & \vdots \\ 0 & 0 & \dots & 1 & \dots & 0 \end{bmatrix} \quad (2)$$

View Return Vector Q : This is a $k \times 1$ vector representing the specific expected returns for each view. It captures the expected return for each individual view from the investor's perspective. If we have forecasted the returns of k stocks to be R_1, R_2, \dots, R_k , the Q matrix can be represented as:

$$Q = \begin{bmatrix} R_1 \\ R_2 \\ \vdots \\ R_k \end{bmatrix} \quad (3)$$

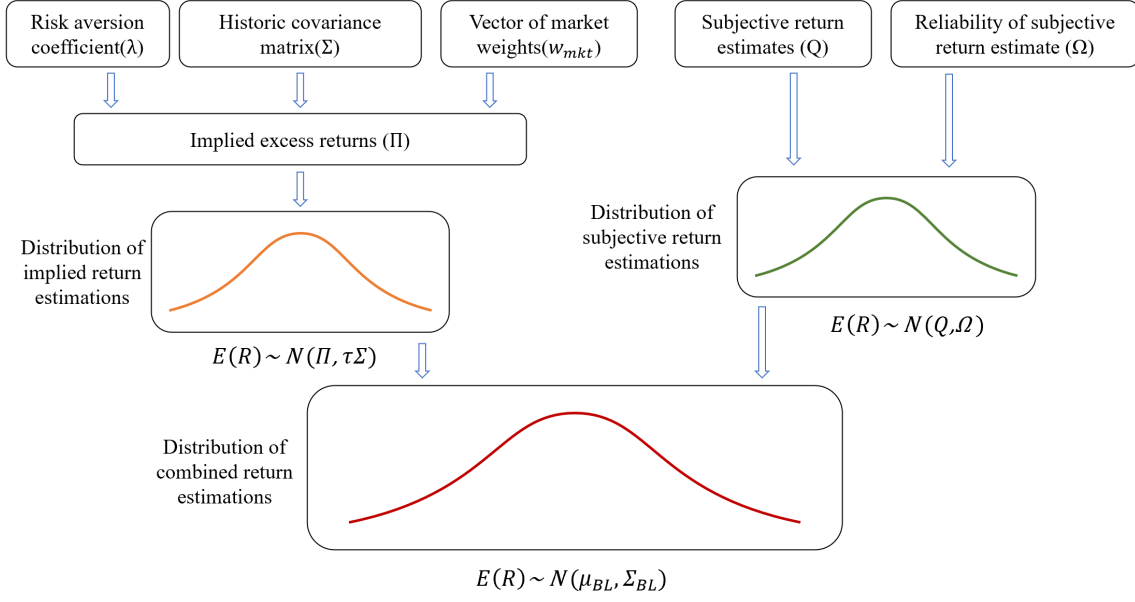


Fig. 1. The process of Black-Litterman model [7].

View Error Covariance Matrix Ω : The view error covariance matrix Ω is a $k \times k$ diagonal matrix representing each view's uncertainty or confidence level. The elements along the diagonal represent the variance for each view, reflecting the investor's confidence in that view. When setting up the Ω matrix, we need to determine a scalar τ . In this example, we use 500 days of historical data for calculating the assets' priori returns and priori covariances and therefore choose $\tau = 1/500$.

$$\Omega = \begin{bmatrix} (p_1 \Sigma p_1') \tau & 0 & \cdots & 0 \\ 0 & (p_2 \Sigma p_2') \tau & \cdots & 0 \\ \vdots & \vdots & \ddots & \vdots \\ 0 & 0 & \cdots & (p_k \Sigma p_k') \tau \end{bmatrix} \quad (4)$$

where, p_i is the asset weight vector for the i -th view, reflecting the investor's assessment of that asset's importance or weight in the view. Σ is the covariance matrix of asset returns, indicating the correlations and volatilities of the asset returns.

3) *Calculating Posterior Returns:* The priori return distribution and the subjective view distribution are combined using Bayesian methods to calculate the posterior estimate of asset expected returns, as shown below:

$$\mu_{post} = \left((\tau\Sigma)^{-1} + P^T \Omega^{-1} P \right)^{-1} \left((\tau\Sigma)^{-1} \Pi + P^T \Omega^{-1} Q \right) \quad (5)$$

And the formula for the posterior covariance (Σ_{post}) is:

$$\Sigma_{post} = \Sigma + \left((\tau\Sigma)^{-1} + P^T \Omega^{-1} P \right)^{-1} \quad (6)$$

4) *Optimizing Asset Allocation:* The posterior returns and the posterior covariance matrix are input into the mean-variance model for optimization to obtain the specific asset allocation weights w_{bl} , as shown below:

$$w_{bl} = (\lambda \Sigma_{post})^{-1} \mu_{post} \quad (7)$$

B. Multivariate Aligned Empirical Mode Decomposition

MA-EMD is an improved version of MEMD, aiming to solve the problems in multivariate decomposition, such as degradation of decomposition quality and computational inefficiency. In MA-EMD, each variable is independently decomposed by the standard EMD to produce a series of IMFs. However, EMD leads to different IMFs for each variable, which the KLD-based frequency alignment module can solve. The main task of this module is to use the extreme value intervals of IMFs to characterize their frequency properties and then measure the similarity of the two IMFs using the Kullback-Leibler Divergence (KLD). Finally, frequency alignment is achieved by assigning each IMF of the related variable (OHLV) to the IMF of the target variable (Close) with the smallest KLD.

1) *EMD Algorithm:* Empirical Mode Decomposition (EMD) is an adaptive signal processing technique suitable for nonlinear and non-stationary signals. Its core is decomposing complex signals into a set of IMFs with different time scales. The first step is to determine the local extreme values of the signal $x(t)$ and use spline interpolation to generate the upper envelope $u(t)$ and the lower envelope $l(t)$. Then calculate the average value $m(t)$ of the two envelopes:

$$m(t) = \frac{u(t) + l(t)}{2} \quad (8)$$

Following this, the mean envelope is subtracted from the original signal to obtain the intrinsic mode function (IMF):

$$h(t) = x(t) - m(t) \quad (9)$$

A qualified IMF must verify that $h(t)$ satisfies two conditions. First, the meaning of the upper and lower envelopes must be zero. Second, the difference between the number of extreme values and the number of zero crossings of $h(t)$ must not exceed 1. If these two conditions are not met, the iterative

decomposition process continues until the conditions are met. After the decomposition is completed, the original signal $x(t)$ can be expressed as the sum of multiple IMFs and a residual term.

$$x(t) = \sum_{i=1}^n h_i(t) + r_n(t) \quad (10)$$

2) *Frequency Alignment Module*: The algorithm uses the spacing between extreme values as a frequency representation method. The extreme value spacing distribution is sufficient for high-frequency IMFs. However, as the extreme values become more and more sparse, the applicability of this indicator for low-frequency IMFs gradually decreases. Cai and Li [49] concluded that partial decomposition does not degrade the performance of the decomposition ensemble model. Therefore, the MA-EMD algorithm stops the decomposition process by setting a threshold ω of the number of extreme values. In this paper, we take $\omega = 20$.

The module uses Kullback-Leibler divergence (KLD) to measure the similarity between the distributions of the extreme value intervals of two IMFs. Before calculating the KLD value, the probability distribution of each IMF needs to be expanded to include all possible extreme value intervals for each IMF. Then, Laplace smoothing is applied to ensure that the probabilities are not zero. The calculation formula is as follows:

$$P'(X = x) = \begin{cases} \frac{N_x}{N-1} + \epsilon, & \text{if } x \in \mathcal{X} \\ \epsilon, & \text{if } x \in \mathcal{X}' \setminus \mathcal{X} \end{cases} \quad (11)$$

where: N_x refers to the number of occurrences of the mechanism interval x in the IMF; N is the total number of extrema points; \mathcal{X} is the set of extrema intervals that exist in this particular IMF; \mathcal{X}' represents the set of extended extrema intervals across all IMFs; ϵ is a very small constant, $\epsilon = 0.000001$.

The final probability distribution $P''(X = x)$ and the formula for calculating the similarity between distributions using KLD are given by Eqs. 12 and 13, respectively.

$$P''(X = x) = \frac{P'(X = x)}{\sum_{x \in \mathcal{X}'} P'(X = x)} \quad (12)$$

$$D_{KL}(P'' \parallel Q'') = \sum_{x \in \mathcal{X}} P''(x) \log \frac{P''(x)}{Q''(x)} \quad (13)$$

where P and Q represent the probability distributions for the related variable and the target variable, respectively, and \mathcal{X} is the extended range of the two distributions.

C. Temporal Convolutional Network (TCN)

TCN is a deep learning model specialized in processing time series data. Its design is inspired by Convolutional Neural Networks (CNNs) structure and optimized and improved for time series prediction tasks. The core innovation of TCN is the combination of dilated convolution and causal convolution techniques.

1) *Causal Convolution*: Causal convolution is one of the core components of TCN, ensuring that the network uses only the current and past information for predictions, without leaking any future information. In causal convolution, the convolution operation is performed only on the current time step and the data before it, achieved by adding zero-padding to the input data. For a one-dimensional sequence input $x \in \mathbb{R}^n$ and a convolutional filter $f : \{0, \dots, k-1\} \rightarrow \mathbb{R}$, the causal convolution operation F at the s -th element of the sequence is defined as:

$$F(s) = (x * f)(s) = \sum_{i=0}^{k-1} f(i) \cdot x_{s-i} \quad (14)$$

where, k is the size of the convolutional kernel, and s is the index of the current time step. This convolution ensures that the output $F(s)$ depends only on x_0, \dots, x_s , and not on future inputs x_{s+1}, \dots, x_n .

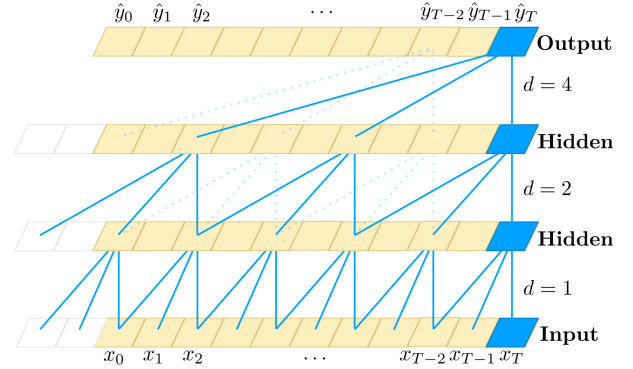


Fig. 2. A dilated causal convolution with dilation factors $d = 1, 2, 4$ and filter size $k = 3$ [50].

2) *Dilated Convolution*: Dilated convolution introduces a skip interval in the convolutional kernel, allowing the receptive field of TCN to grow exponentially. For example, when the dilation factor is 2, the convolution kernel skips one data point during the convolution operation. As the network depth increases, the dilation factor gradually increases, enabling the network to capture longer temporal dependencies, as shown in Fig. 2. For a dilation factor d , the dilated convolution operation F_d at the s -th element of the sequence is defined as:

$$F_d(s) = (x *^d f)(s) = \sum_{i=0}^{k-1} f(i) \cdot x_{s-d \cdot i} \quad (15)$$

where d is the dilation factor, and k is the size of the convolutional kernel.

3) *Residual Connections*: To alleviate the issues of vanishing and exploding gradients during the training of deep networks, TCN introduces residual connections. Residual connections make it easier for the network to learn identity mappings by directly adding the input to the output. In TCN, each residual block typically consists of two dilated convolution layers, weight normalization, ReLU activation functions, and a dropout layer. If the dimensions of the input and output are not consistent, a 1×1 convolution can be used to adjust the dimensions to allow for element-wise addition. As shown in

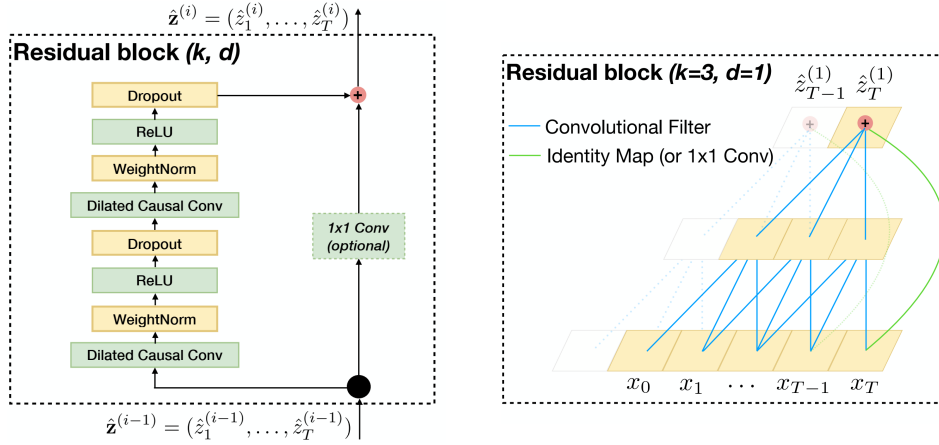


Fig. 3. The residual block in TCNs. Left plot: an 1×1 convolution is added when the residual input and output have different dimensions. Right plot: an example of the residual connection in TCN [50].

Fig. 3. For an input x and the output of a convolutional layer $F(x)$, the output of a residual block o is:

$$o = \text{Activation}(x + F(x)) \quad (16)$$

where Activation is a nonlinear activation function, such as ReLU.

D. Singular Spectral Analysis (SSA)

SSA is a classic method for processing time series data. It embeds data into a high-dimensional space and uses a sliding window combined with singular value decomposition (SVD) to extract the main patterns.

The first step of SSA involves reconstructing the time series into a matrix containing lagged vectors. Starting with a time series of length N , denoted as $\{x_1, x_2, \dots, x_N\}$, a window size L is selected, typically much smaller than N (usually $L < N/2$). This window is used to construct a trajectory matrix X , which has L rows and $K = N - L + 1$ columns. The matrix X is built by sliding the window across the time series, with each row representing a "snapshot" of the series at a given time point. The structure of the time series over time is thus captured in this matrix:

$$X = \begin{bmatrix} x_1 & x_2 & \dots & x_K \\ x_2 & x_3 & \dots & x_{K+1} \\ \vdots & \vdots & \ddots & \vdots \\ x_L & x_{L+1} & \dots & x_N \end{bmatrix} \quad (17)$$

With the trajectory matrix in hand, the next step is to decompose it further using SVD. SVD is a technique that breaks down the matrix into three parts: two orthogonal matrices and a diagonal matrix containing the singular values. The SVD of matrix X is expressed as:

$$X = U \Sigma V^T \quad (18)$$

where $U \in \mathbb{R}^{L \times L}$ contains the left singular vectors, $\Sigma \in \mathbb{R}^{L \times K}$ is the singular value matrix with diagonal values representing the strength of each component, and $V^T \in \mathbb{R}^{K \times K}$ contains the right singular vectors.

Following the decomposition, the time series is divided into multiple linearly independent subseries through grouping. The singular values $\{\sigma_1, \sigma_2, \dots, \sigma_r\}$ are partitioned into m groups $\{I_1, I_2, \dots, I_m\}$, with each group corresponding to a submatrix. For the i -th group, the submatrix X_i is formed by multiplying the corresponding singular values, left singular vectors, and right singular vectors:

$$X_i = \sum_{j=1}^{k_i} \sigma_{i_j} u_{i_j} v_{i_j}^T \quad (19)$$

where u_{i_j} and v_{i_j} are the i_j -th columns of U and V , respectively.

The final step involves reconstructing the time series from the grouped submatrices. Anti-diagonal averaging is performed on each submatrix to obtain the reconstructed series. For each group $\{I_1, I_2, \dots, I_m\}$, the corresponding submatrix X_i is averaged along the anti-diagonals to produce a sequence \hat{y}_i of length $N = L + K - 1$. The formula for anti-diagonal averaging is:

$$\hat{y}_i(k) = \frac{1}{n_k} \sum_{j=1}^{n_k} X_i(j, k - j + 1) \quad (20)$$

where n_k is the number of elements on the k -th anti-diagonal. The reconstructed original time series \hat{Y}_N is obtained by summing these sequences:

$$\hat{Y}_N = \sum_{i=1}^m \hat{y}_i \quad (21)$$

This reconstruction process combines the decomposed subseries to produce a denoised version of the original time series.

IV. EXPERIMENT DESIGN

A. Data description

To construct an investment portfolio, we carefully selected 20 representative stocks from various industries within the NASDAQ 100 index as the targets for our portfolio. These stocks cover key areas such as technology, healthcare, and

consumer sectors and are known for their high growth potential and innovative capabilities, as shown in Table I. We collected the daily trading data of these stocks from January 1, 2020, to August 31, 2023, from Yahoo Finance.

TABLE I
STOCK POOL FOR PORTFOLIO CONSTRUCTION

Stock	Sector	Stock	Sector
AAPL	Technology	COST	Consumer Discretionary
MSFT	Technology	AZN	Health Care
GOOG	Technology	AMGN	Health Care
GOOGL	Technology	ISRG	Health Care
NVDA	Technology	PEP	Consumer Staples
INTC	Technology	HON	Industrials
AMD	Technology	LIN	Industrials
AMZN	Consumer Discretionary	TMUS	Telecommunications
TSLA	Consumer Discretionary	CMCSA	Telecommunications
NFLX	Consumer Discretionary	CSCO	Telecommunications

Among the 20 stocks, we focus on eight key stocks, including Apple (AAPL), Microsoft (MSFT), Alphabet Class A (GOOGL), Nvidia (NVDA), Tesla (TSLA), Amgen (AMGN), PepsiCo (PEP), and Honeywell International (HON). These stocks hold significant market positions in their respective sectors, and detailed statistical analyses are presented in Table II.

TABLE II
THE STATISTICAL ANALYSIS RESULTS OF SELECTED STOCKS

Stock	Max	Min	Mean	Std
AAPL	194.757660	54.449886	134.691305	32.169206
MSFT	354.635529	129.621140	248.133411	50.025388
GOOGL	149.125549	52.455711	104.987753	24.722698
NVDA	49.332607	4.892426	18.843253	9.475752
TSLA	409.970001	24.081333	206.142350	88.800801
AMGN	270.247192	156.284851	213.201788	18.757325
PEP	185.979691	90.621956	144.517614	21.378415
HON	217.264450	93.658630	179.906142	25.235809

B. Proposed Methodology

In this paper, we propose a novel stock price prediction model, SSA-MAEMD-TCN, and consider the model as a way to enhance the subjective view of the investor and thus optimize the performance of Black-Litterman's portfolio. See Fig. 4 for the overall framework.

Predict stock prices: This stage aims to predict stock prices using a hybrid model. First, the original time series data are subjected to SSA denoising to reduce the noise interference. The denoised data are then decomposed into multiple IMFs using MA-EMD, as shown in Fig. 5, where it can be visualized that the number of IMFs for each variable is equivalent. Before decomposition, normalizing the data is not negligible, as shown in the following equations:

$$z_{t,i} = \frac{x_{t,i} - \mu_i}{\sigma_i} \quad (22)$$

Where, $x_{t,i}$ is the raw value of the i -th feature at time t . μ_i is the mean of the i -th feature, σ_i is the standard deviation of the i -th feature.

The final step of the prediction framework is to predict the IMF for each alignment using a TCN. We use the sliding

window method to divide the data into many short time intervals using a fixed-length seven-step input, with the eighth data point serving as a label. The window gradually moved forward until the last window reached. Regarding the division of the dataset, 70% of the data is assigned to the training set, 15% to the validation set, and the remaining 15% as the test set (out-of-sample data). Finally, the predicted values of each IMF are summed up to give the final prediction. See Table III for specific parameters of the model.

TABLE III
HYPERPARAMETER TUNING FOR TCNS.

Hyperparameter	Chosen Value
Kernel_sizes	2
Hidden_size	[64, 128]
Learning_rate	0.001
Layer_num	2
Dropout_rate	[0, 0.3]
Epochs	[50, 100]
Batch_size	[16, 32]
Activation function	ReLU
Optimizer	Adam

Construct the portfolio: The next step is to calculate the market equilibrium return based on inputs such as market capitalization, daily return rate, and risk-free rate. Inverse optimization is used to obtain the equilibrium return after determining the risk aversion coefficient and constructing the covariance matrix. The asset prices predicted in the first stage are converted into returns to generate subjective opinions. Finally, the posterior excess return and posterior covariance are obtained according to Eqs. 5 and 6, and the optimized portfolio weights are obtained using Eq. 7.

C. Assessment metric

1) *Predictive model evaluation metrics:* To evaluate the performance of the proposed hybrid model, we employ three metrics for assessment: RMSE, MAPE, and the R^2 , based on Eqs. (23, 24, 25). RMSE measures the difference between the predicted and actual values; the smaller the value, the closer the model's prediction is to the exact value. MAPE expresses the error as a percentage, mainly reflecting the difference between the predicted and actual values. R^2 measures the model's goodness of fit, and its value ranges from 0 to 1. The closer the value of R^2 to 1, the better the model's fit to the data.

$$RMSE = \sqrt{\frac{1}{N} \sum_{t=1}^N (y_t - \hat{y}_t)^2} \quad (23)$$

$$MAPE = \frac{1}{N} \sum_{t=1}^N \left| \frac{y_t - \hat{y}_t}{y_t} \right| \times 100\% \quad (24)$$

$$R^2 = 1 - \frac{\sum_{t=1}^N (y_t - \hat{y}_t)^2}{\sum_{t=1}^N (y_t - \bar{y})^2} \quad (25)$$

In the aforementioned formula, y_t denotes the actual value, \hat{y}_t denotes the predicted value, \bar{y} is the mean of the actual values, and N represents the total number of samples.

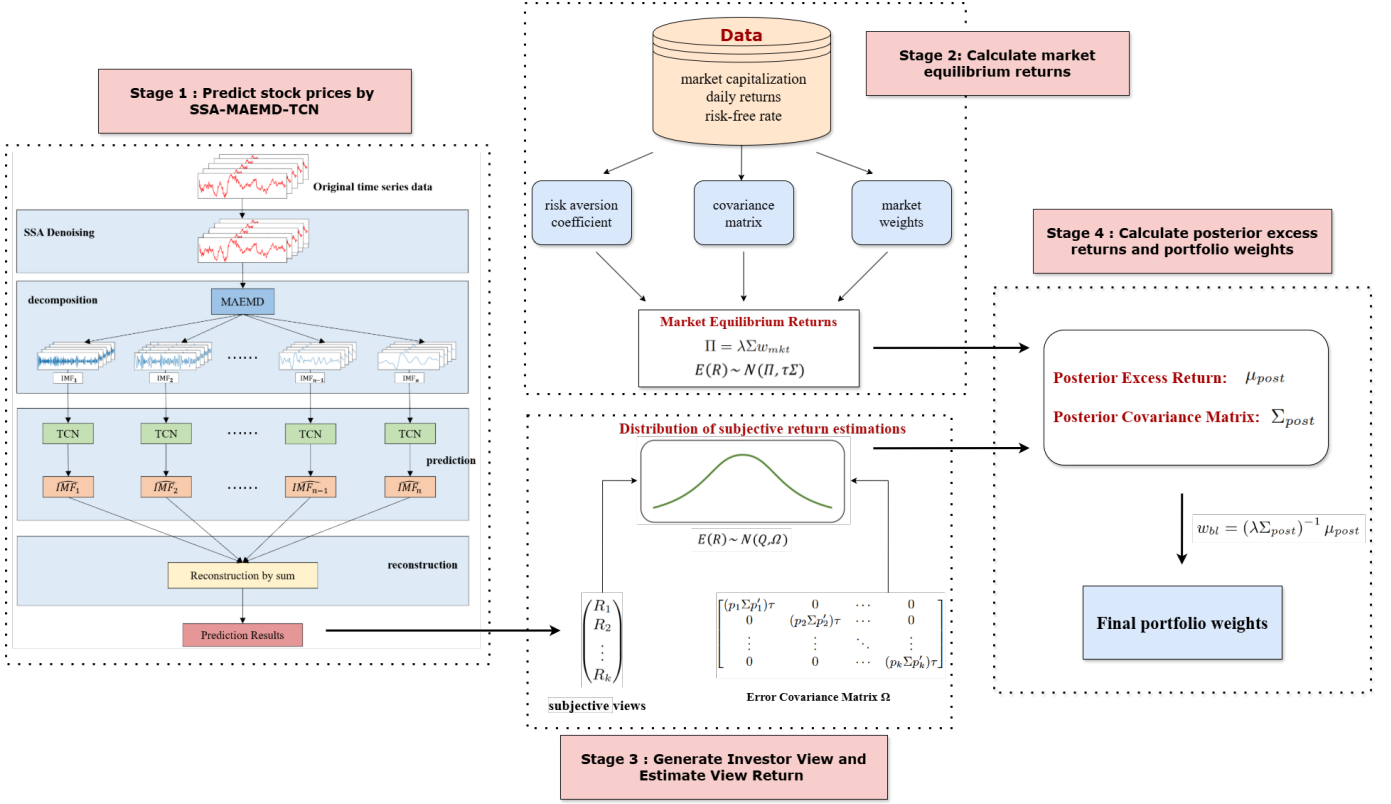


Fig. 4. Procedure of the complete Black-Litterman strategy.

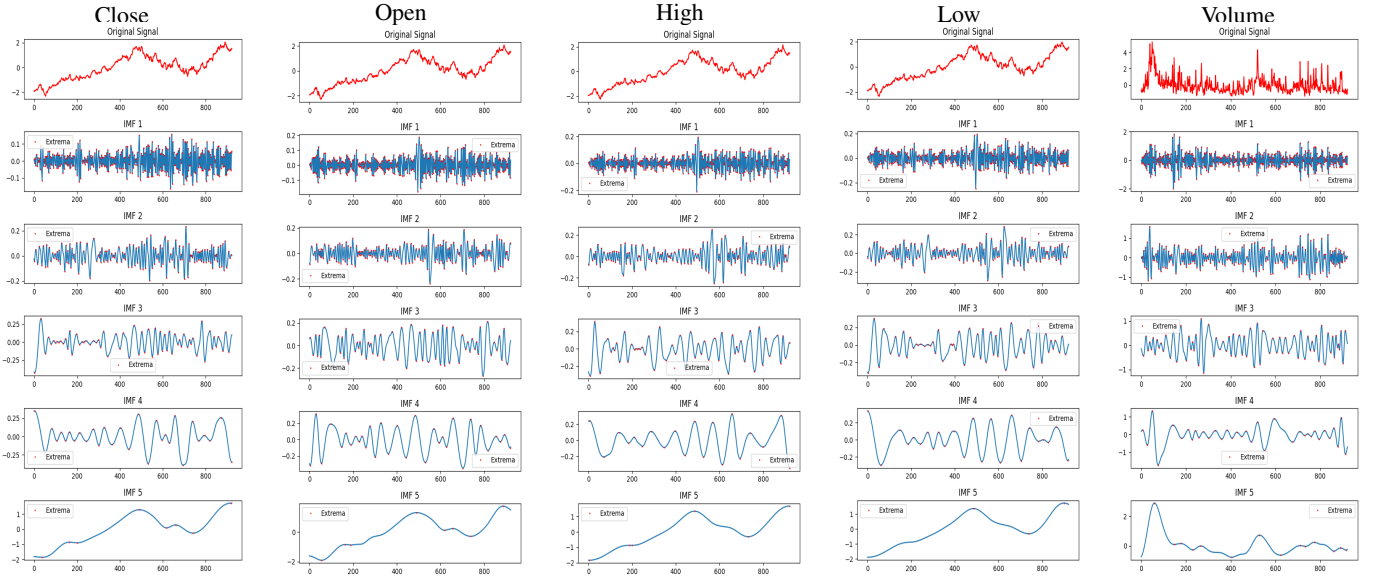


Fig. 5. COHLV of MSFT was decomposed using MA-EMD.

2) *Portfolio evaluation metrics*: The Sharpe Ratio is a commonly used metric in finance for measuring the performance of investment portfolios. It assesses the risk-adjusted return of a portfolio, that is, the excess return per unit of total risk.

$$\text{Sharpe Ratio} = \frac{R_p - R_f}{\sigma_p} \quad (26)$$

where, R_p is the expected return of the portfolio. R_f is the risk-free rate. σ_p is the standard deviation of the portfolio's

returns, representing the total risk.

The Herfindahl-Hirschman Index (HHI) is used to quantify the concentration and diversification of a portfolio. The HHI reflects the concentration of a portfolio by adding the squares of the weights of each asset in the portfolio. The lower the HHI value, the more diversified the portfolio is.

$$\text{HHI} = \sum_{i=1}^n (w_i)^2 \quad (27)$$

TABLE IV
PREDICTION ACCURACY OF DIFFERENT MODELS.

		Model-1	Model-2	Model-3	Model-4
AAPL	RMSE	1.56289030	1.93084338	2.36024831	2.94097123
	MAPE	0.00755294	0.00893367	0.01085755	0.01251939
	R ²	0.98664278	0.97958137	0.96740712	0.94912388
MSFT	RMSE	2.91770909	3.35597227	4.45542509	5.40041018
	MAPE	0.00779198	0.00830468	0.01223130	0.01391688
	R ²	0.98989646	0.98663039	0.97647335	0.96516374
GOOGL	RMSE	1.13545415	1.76281289	2.12105377	1.90920327
	MAPE	0.00798771	0.01188872	0.01536526	0.01374732
	R ²	0.99192566	0.98054508	0.97157358	0.97724051
NVDA	RMSE	0.85905343	0.96575539	1.36083967	1.57894392
	MAPE	0.02150728	0.02178651	0.02522960	0.03223496
	R ²	0.98994983	0.98763062	0.97529373	0.96235317
TSLA	RMSE	4.42258848	5.66938133	5.44426940	5.95044438
	MAPE	0.01377828	0.02061087	0.02200192	0.02209831
	R ²	0.98739496	0.97926430	0.98090015	0.97714708
AMGN	RMSE	1.43078840	2.53478284	2.95386690	3.65689368
	MAPE	0.00496882	0.00880632	0.01200920	0.01290778
	R ²	0.98660679	0.95790873	0.94291580	0.91239135
PEP	RMSE	1.04521062	2.15265476	1.68072212	2.27383710
	MAPE	0.00474268	0.01043224	0.00801190	0.01050823
	R ²	0.96524834	0.85331936	0.91058387	0.82263936
HON	RMSE	1.24145865	1.38090183	1.48163104	1.84781323
	MAPE	0.00501248	0.00579047	0.00626205	0.00746165
	R ²	0.96035549	0.95075333	0.94353249	0.91217170

Model-1: SSA-MAEMD-TCN, Model-2: MAEMD-TCN,
Model-3: MEMD-TCN, Model-4: MAEMD-LSTM

where w_i represents the weight of the i -th stock, and n is the total number of stocks in the market.

V. RESULT DISCUSSION

A. Prediction results

In this section, we perform a comprehensive comparative analysis of the proposed SSA-MAEMD-TCN hybrid model with the benchmark models (MAEMD-TCN, MEMD-TCN, MAEMD-LSTM) to evaluate their performance in stock price prediction tasks. We used three evaluation metrics: RMSE, MAPE and R². These metrics can reflect the predictive accuracy and goodness-of-fit of the models from different perspectives.

From the data in Table IV, SSA-MAEMD-TCN is significantly better than MAEMD-TCN for all the stocks. For example, the RMSE of the former is 1.1355 in GooGL, while that of the latter is 1.7628, and the predicted values of SSA-MAEMD-TCN are closer to the actual values. The former also shows better performance in terms of MAPE and R². In addition, the prediction performance of SSA-MAEMD-TCN is better than that of all the benchmark models mentioned above. The advantage of the proposed model is the introduction of SSA for data preprocessing and noise reduction. This step dramatically reduces the impact of noise in financial data on subsequent predictions, enabling the model to accurately capture valid information in the data and improve the overall prediction results. Thus, the use of SSA for data preprocessing is necessary.

TABLE V
LEARNING ABILITY OF MODELS FOR HIGH-FREQUENCY IMFS.

Stock	Model-1			Model-2		
	IMF	RMSE	R ²	IMF	RMSE	R ²
AAPL	IMF_1	0.015491	0.852987	IMF_1	0.036864	-0.420059
	IMF_2	0.005227	0.992064	IMF_2	0.012167	0.942352
	IMF_3	0.004628	0.997790	IMF_3	0.004540	0.996048
MSFT	IMF_1	0.012974	0.926302	IMF_1	0.054744	-2.954987
	IMF_2	0.007164	0.986296	IMF_2	0.018356	0.891233
	IMF_3	0.008833	0.993311	IMF_3	0.010355	0.981963
GOOGL	IMF_1	0.018124	0.889961	IMF_1	0.039699	-0.339571
	IMF_2	0.008130	0.986513	IMF_2	0.013028	0.943667
	IMF_3	0.008081	0.995408	IMF_3	0.007523	0.990632
NVDA	IMF_1	0.015683	0.781492	IMF_1	0.039973	-0.605121
	IMF_2	0.006152	0.985119	IMF_2	0.010219	0.943378
	IMF_3	0.009285	0.990885	IMF_3	0.008411	0.987382
TSLA	IMF_1	0.021752	0.825375	IMF_1	0.030998	0.535461
	IMF_2	0.006575	0.994365	IMF_2	0.012492	0.946684
	IMF_3	0.010453	0.993085	IMF_3	0.007014	0.993969
AMGN	IMF_1	0.033340	0.862009	IMF_1	0.061505	0.597144
	IMF_2	0.012138	0.992682	IMF_2	0.027600	0.945031
	IMF_3	0.015334	0.993429	IMF_3	0.014064	0.991653
PEP	IMF_1	0.017327	0.753860	IMF_1	0.034134	0.109507
	IMF_2	0.004800	0.988180	IMF_2	0.011979	0.943010
	IMF_3	0.006032	0.996796	IMF_3	0.006712	0.990697
HON	IMF_1	0.023546	0.852260	IMF_1	0.045713	0.308172
	IMF_2	0.008809	0.991676	IMF_2	0.012854	0.960596
	IMF_3	0.010923	0.995635	IMF_3	0.006662	0.995651

MAEMD-TCN outperforms MEMD-TCN in the prediction of most of the stocks. In the case of AAPL, for example, the RMSE of MAEMD-TCN is 1.9308, which is lower than that of MEMD-TCN (2.3602). Regarding MAPE, the value of MAEMD-TCN is 0.0089, which is lower than that of MEMD-TCN (0.0109), indicating that its prediction error is minor. R² also shows that the fit of the MAEMD-TCN model (0.9796) to the data is better than that of MEMD-TCN (0.9674). MAEMD solves the problem of the deficiency of MEMD in multivariate decomposition. Secondly, it uses KLD to evaluate the frequency similarity of different variable IMFs to ensure the consistency and matching of the decomposed IMFs in frequency. This improved decomposition method provides TCN with higher-quality input features, enabling MAEMD-TCN to capture patterns and regularities in time series accurately.

In comparing MAEMD-LSTM and MAEMD-TCN, the later shows advantages in all three metrics. Compared with LSTM, the advantage of TCN is that it can effectively extend the sensory field to capture long-distance dependencies in time series, is less prone to the problem of gradient vanishing or gradient explosion during the training process, and has a more stable prediction performance. Therefore, MAEMD-TCN can more effectively extract the time series' short-range and long-range dependency features, thus realizing more accurate prediction results.

The following section will analyze how the noise reduction step improves the model performance. The EMD-based decomposition algorithm decomposes the sequence into multiple IMFs, and the forecasting model outputs the forecast values

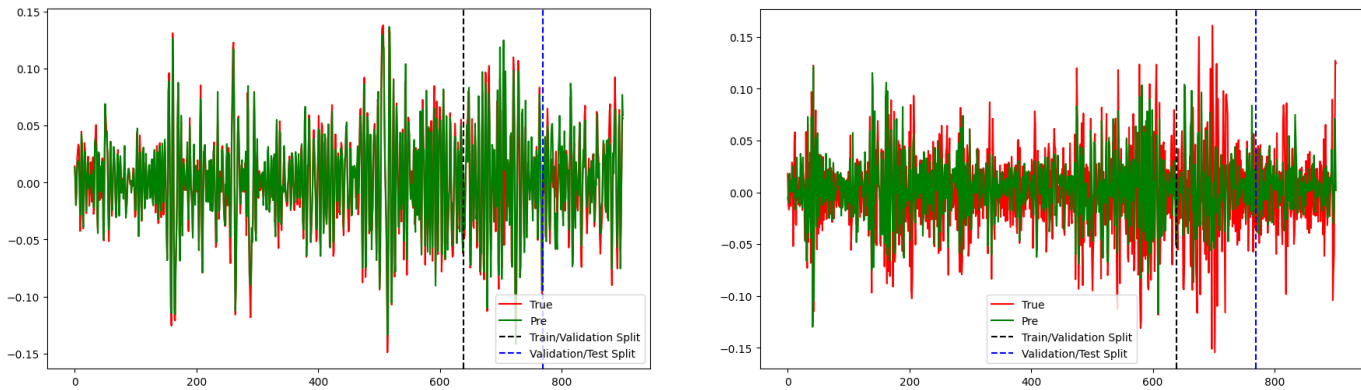


Fig. 6. Effectiveness of different models in fitting IMF_1 of AAPL (The data has not been denormalized).

of these components and integrates them. The high-frequency components (such as IMF_1) contain a lot of noise, which will interfere with the model’s learning of effective trends. Through SSA denoising, SSA-MAEMD-TCN significantly outperforms MAEMD-TCN in predicting high-frequency components. As shown in Table V, RMSE and R^2 indicators represent the model’s learning ability, and Figure 6 visualizes the fitting effect of SSA-MAEMD-TCN and MAEMD-TCN on the high-frequency IMFs using AAPL as an example.

In IMF_1 of AAPL, RMSE decreased from 0.036864 to 0.015491 (58.0%), and MSFT from 0.054744 to 0.012974 (76.3%). The R^2 indicator also improved significantly, from -0.339 to 0.890 in the GOOGL data. The denoising effect still exists in the sub-high frequency component (IMF_2), but the improvement is weakened. For example, the RMSE of NVDA is reduced by 39.8%, and the R^2 of GOOGLE is improved by 3.23%. The noise impact is already low in the intermediate frequency component (IMF 3), and the denoising optimization effect is limited.

These results show that the SSA denoising step effectively separates high-frequency noise from trend information, allowing the model to more accurately capture the trend characteristics in the sequence, thereby improving the overall prediction performance.

We can draw the following conclusions by analyzing the overall prediction performance and comparing the learning ability for high-frequency components.

- 1) **MA-EMD outperforms MEMD:** MA-EMD enhances the quality and consistency of IMFs through a frequency alignment module, addressing MEMD’s limitations in multivariate decomposition and providing superior input features for prediction models.
- 2) **TCN is superior to LSTM:** TCN effectively uses its receptive field to capture long-range dependencies in time series and ensures more stable training, enabling better extraction of short—and long-term features.
- 3) **SSA is essential for data denoising:** The ability of SSA to filter out noise interference provides higher-quality inputs for subsequent decomposition and prediction steps, significantly improving the model’s prediction performance in high-frequency components and optimizing the overall prediction results.

B. Portfolio Optimization

In this section, we construct investor views based on the prediction results of the proposed model for eight stocks and construct an investment portfolio through the BL model. We select 132 trading days from February 23, 2023, to August 31, 2023 (out-of-sample data in the previous section) as the back-testing period. We select the mean-variance model (MV), the equal-weight model (EW), and the market-weighted portfolio model (MW) as benchmark models. This paper adopts two backtesting methods: “rolling data scheme” and “rebalancing strategy.” In addition, we also compare the weight distribution of the portfolios constructed by the BL model and the MV model to evaluate whether the BL model can make up for the shortcomings of the MV model.

1) *Rolling data scheme:* This study uses a rolling data scheme to assess the effectiveness of portfolios under different holding periods. Starting from the initial date of the specified test period, the portfolio is constructed based on the forecast data of that day. It is assumed to remain unchanged for a predetermined holding period (e.g., 10 days). After the first holding period, the portfolio is reconstructed using forecast data from the second day of the test period, and the process is repeated until the end of the test period. The portfolio’s overall performance is assessed by calculating and annualizing the average return over the holding period, which is taken to be 1, 3, 5, 10, and 20 days. The focus is on observing the relationship between annualized returns and Sharpe ratios and the length of the holding period.

The empirical results in Fig. 7 confirm the significant advantages of the BL model for short holding periods. When looking at the overall data, all strategies exhibit high Sharpe ratios and decent annualized returns under different holding periods, indicating that the market is in a state where the trend is more pronounced or the volatility is relatively orderly, giving all investment strategies a chance to achieve profitability.

With a holding period of 1 day, the BL model achieves an annualized return of more than 80% and a Sharpe ratio of about 4.5, which significantly outperforms the other models. This is mainly due to the proposed hybrid model, which improves the accuracy of the subjective view. By keenly capturing market fluctuations, the BL model adequately adjusts the portfolio, resulting in high returns and better

TABLE VI
THE NUMBER OF TIMES WITH THE HIGHEST AND LOWEST RETURN AT ROLLING RUNS.

Holding period	Number of Runs	Highest Return				Lowest Return			
		BL-Highest	EW-Highest	MW-Highest	MV-Highest	BL-Lowest	EW-Lowest	MW-Lowest	MV-Lowest
1	132	53 (40.15%)	24	1	54	7 (5.30%)	22	49	54
3	130	55 (42.31%)	20	10	45	7 (5.38%)	40	32	51
5	128	40 (31.25%)	19	14	55	14 (10.94%)	32	31	51
10	123	28 (22.76%)	25	22	48	8 (6.50%)	46	24	45
20	113	26 (23.01%)	25	24	38	14 (12.39%)	29	26	44
Overall	626	202	113	71	240	50	169	162	245
Percentage		32.27%	18.05%	11.34%	38.34%	7.99%	27.00%	25.88%	39.14%

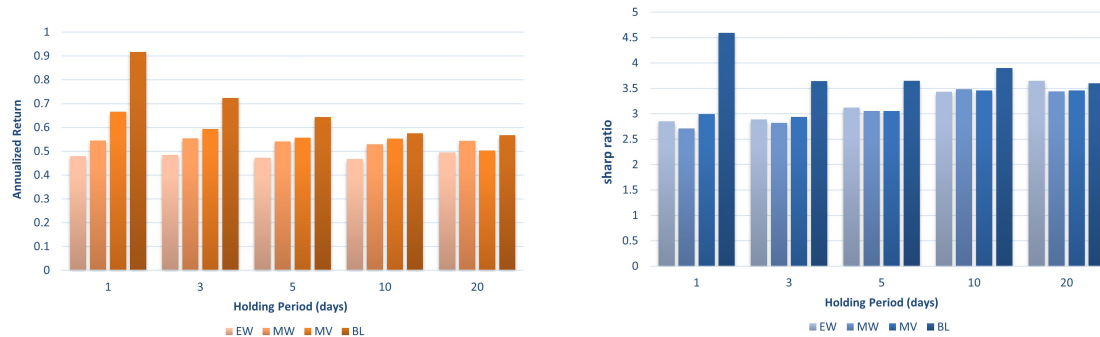


Fig. 7. Evaluate portfolio performance using annualized returns and Sharpe ratios.

risk control during the short holding period. As the holding period lengthens, the advantages of BL's annualized returns and Sharpe ratios diminish. Longer periods increase market uncertainty, and subjective views are no longer adapted to market conditions. Based on these outdated views, portfolio adjustments are no longer effective, and yield and volatility control advantages are no longer as pronounced in the short term.

To further verify the above experimental findings, we count the times the four models obtain the highest return and the times they get the lowest return under different holding periods, as shown in Table VI. For the 1-day and 3-day holding periods, the BL model obtains the highest return 53 times and 55 times, accounting for 40.15% and 42.31%, respectively. In contrast, the lowest returns are only 7 times, 5.30% and 5.38%, highlighting its stability and superiority in short-term investment. When the holding period is gradually extended, the number of times that the BL model obtains the highest rate of return gradually decreases, and the number of times that it obtains the lowest rate of return gradually increases, especially when the holding period is 20 days, it reaches 14 times, accounting for 12.39%, which indicates that its volatility and riskiness increase in a more

2) *Rebalancing Strategy*: The rebalancing strategy dynamically manages an investment portfolio by adjusting asset weights to meet the investor's initial goals. When market fluctuations cause asset weights to deviate from the preset ratio, the target weights are restored by buying and selling assets. This adjustment can be a regular adjustment based on time intervals or an irregular adjustment based on the degree

of deviation of asset weights. This paper uses the "periodic rebalancing strategy" for experiments and assumes that the transaction cost is 0.2%. The holding period is consistent with the previous article. Table VII shows the performance of four different portfolio strategies under different holding periods.

TABLE VII
PERFORMANCE OF PORTFOLIO MANAGEMENT WITH REBALANCING

Period	Metrics	BL	MV	EW	MW
1	Annual Return	1.0335	0.3399	0.5247	0.5951
	Annual Volatility	0.1889	0.2038	0.1508	0.1826
	Sharpe Ratio	4.2154	1.3967	2.8288	2.6629
3	Annual Return	0.7963	0.5411	0.5240	0.5973
	Annual Volatility	0.1748	0.1841	0.1437	0.1731
	Sharpe Ratio	3.6301	2.4209	2.9633	2.8157
5	Annual Return	0.6689	0.5801	0.5236	0.6010
	Annual Volatility	0.1660	0.1466	0.1370	0.1647
	Sharpe Ratio	3.1850	3.1359	3.0292	2.9027
10	Annual Return	0.6056	0.5750	0.5261	0.5996
	Annual Volatility	0.1317	0.1332	0.1174	0.1390
	Sharpe Ratio	3.4953	3.2902	3.4048	3.2879
20	Annual Return	0.6264	0.5322	0.5368	0.5946
	Annual Volatility	0.1424	0.1604	0.1095	0.1386
	Sharpe Ratio	3.3877	2.5836	3.7542	3.3066

The BL model shows a significant holding period effect: when the holding period is extended from 1 day to 20 days, the expected annualized return decreases from 1.0335 to 0.6264, and the Sharpe ratio decreases from 4.2154 to 3.3877. It is the only strategy whose Sharpe ratio decreases with the increase of the holding period. This shows that the BL model achieves higher returns in a short holding period

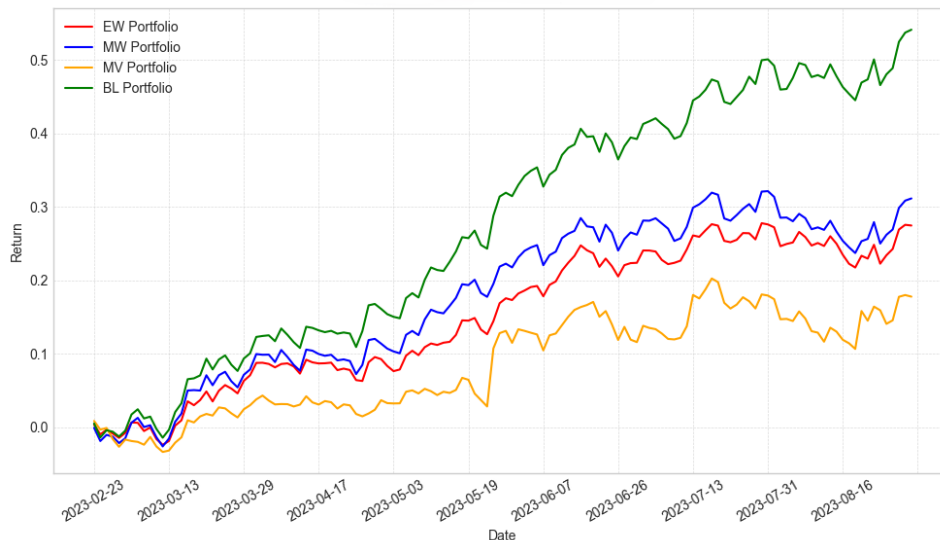


Fig. 8. Cumulative return of 1-day rebalancing.

by combining market equilibrium returns and subjective views through a Bayesian framework. Although the transaction costs are high, its excellent performance makes the strategy returns less affected by transaction costs. However, as the holding period increases, the adaptability of investors' views decreases, and the performance of the BL model gradually approaches that of the MW model. The annualized return of the MV model shows a trend of first rising and then falling with the increase of the holding period: from 0.3399 in a 1-day holding period to 0.5801 in a 5-day holding period, and then falls back to 0.5322 in 20 days (a decrease of 7.4%), while the volatility shows a trend of first falling and then rising. In the short holding period, the Sharpe ratio of the MV model is significantly lower than that of the BL model, exposing the problems of high transaction costs and parameter misalignment under high-frequency adjustments.

In contrast, the EW and MW portfolios maintain relatively stable annualized returns under different holding periods, with gradually decreasing volatility and gradually increasing Sharpe ratios, verifying the characteristics of passive allocation to achieve long-term stability by diversifying risks. However, the passive investment strategy lacks flexibility, and its returns and Sharpe ratios are lower than the BL model's in the short holding period (1-3 days).

TABLE VIII
PERFORMANCE OF PORTFOLIO MANAGEMENT WITH 1-DAY REBALANCING

	EW	MW	MV	BL
daily average return (%)	0.1886	0.2124	0.1323	0.3354
daily volatility(%)	0.9498	1.1505	1.2840	1.1900
Cumulative Return	0.2748	0.3117	0.1780	0.5414
Sharpe Ratio	2.8288	2.6629	1.3967	4.2154

We focus on analyzing a special case of the rebalancing strategy: 1-day rebalancing, which is essentially a portfolio model that generates daily portfolio weights, as shown in Table

VIII and Fig. 8. In the framework of this strategy, the BL model has a significantly higher average daily and cumulative return than the other strategies, with a Sharpe ratio of 4.2154, much higher than the MV model's 1.3967. Although the daily volatility of 1.190% is slightly higher than that of the equal-weighted portfolio's 0.9498%, the high Sharpe ratio confirms the effectiveness of this strategy dynamically adjusting to the short holding period. Combined with the accurate prediction results of the hybrid model, the BL model achieves a balance between maximizing return and controlling risk in a very short holding period.

The EW portfolio reflects the defensive nature of the passive strategy with the lowest volatility and stable returns. Still, its cumulative return is only 50% of the BL model's. The MV model has the lowest daily return and the highest daily volatility. These data show that its reliance on historical data for optimization has the risk of overfitting, and the transaction costs of high-frequency position adjustments further weaken the model performance. In short, the BL model is thoroughly dominant in high-frequency active investment strategies.

3) *Portfolio Diversification*: In this section, we discuss the degree of portfolio diversification for the BL and MV models. We select the daily weights under 1-day rebalancing to test whether the BL model has more advantages in asset diversification. As seen from the two-dimensional empirical results of Stock quantity distribution and HHI (Table IX), the BL and the MV models present a significant difference in underlying diversification. In terms of weight distribution, the BL model covers 18.03 stocks with a standard deviation of 1.039, which is significantly better than the MV model's 11.19 stocks. Meanwhile, the former's standard deviation is even lower than that of the latter, suggesting that the BL model has a more stable underlying distribution.

Further deconstructing the concentration difference by HHI, the mean HHI of the BL model is 0.131, which is much lower than that of the MV model (0.245). Its HHI standard

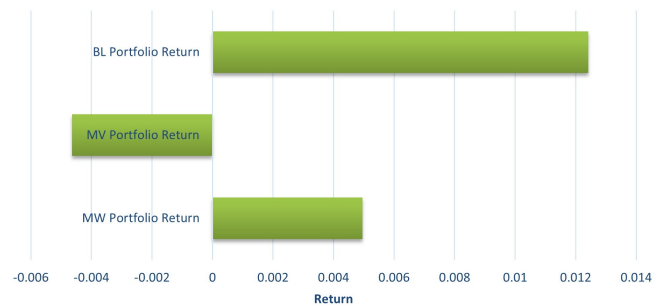
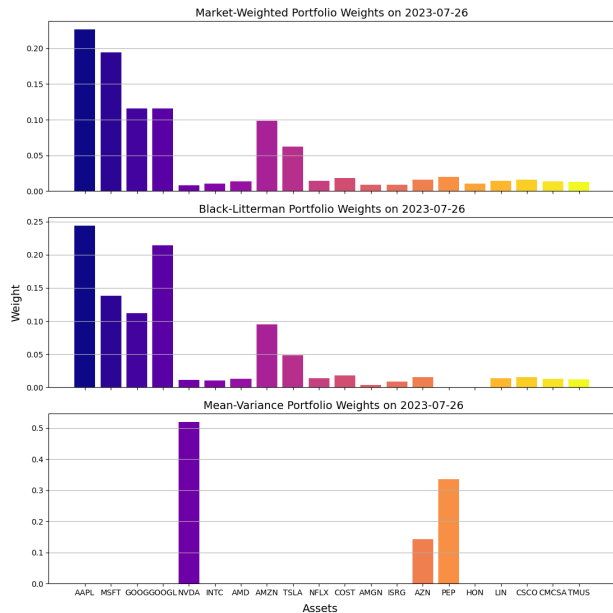


Fig. 9. Comparison of different portfolio weights and returns in 2023.07.26

TABLE IX
PORTFOLIO WEIGHT DISTRIBUTION

	MV	BL
Mean of stock number	11.19	18.03
Std of stock number	8.183	0.937
Mean of HHI	0.245	0.131
Std of HHI	0.157	0.009

deviation is only 0.009, which is equivalent to 5.73% of the volatility of the MV model. The MV model presents high concentration and allocation instability compared to the BL model. Regarding portfolio diversification, the BL model is superior across the board in the diversification and robustness dimensions.

Fig. 9 shows the weights and returns of different investment portfolios on a particular day. The BL model combines the views of investors, so its investment portfolio can be regarded as an optimization of the MW portfolio. Therefore, ideally, the single-day return of the BL model is higher. The portfolio distribution and return of the MV model in this day are not good enough.

VI. CONCLUSION

The traditional Black-Litterman model faces challenges in generating investor opinions. This study innovatively constructs a hybrid deep learning framework of SSA-MAEMD-TCN to achieve high-precision stock price prediction and provide reliable input for the Black-Litterman model. Empirical results show that in terms of asset price prediction, the hybrid model significantly outperforms the three benchmark models MAEMD-TCN, MEMD-TCN, and MAEMD-LSTM in key indicators such as RMSE, MAPE, and R^2 , and SSA denoising

can indeed help the model capture the trend of high-frequency IMFs.

We use two backtesting methods in portfolio management to conduct a comprehensive performance evaluation of the portfolio built based on this model. Compared with benchmark models such as the mean-variance, equal-weighted, and market-weighted models, the portfolio generated by combining the hybrid model with the BL model has high returns and low risks in a short-holding period. As the holding period increases, its performance gradually approaches the market-weighted model. In addition, we examine the degree of portfolio diversification. Compared with the mean-variance model, the BL model can generate a more diversified portfolio, effectively reduce concentration risk, and enhance the portfolio's robustness.

Future research can focus on two main directions. First, the current model mainly relies on daily data for single-step prediction, which is only suitable for short-term transactions. By developing a multi-step prediction model, we can predict stock price trends over an extended period, allowing investors to make informed decisions for medium- and long-term investments. Second, further research is needed to improve portfolio optimization methods, especially in dynamic environments. Techniques such as reinforcement learning and online learning can be explored to develop adaptive portfolio optimization strategies that automatically adjust and optimize according to changing market conditions.

REFERENCES

- [1] H. Markowitz, "Portfolio selection," *The Journal of Finance*, vol. 7, no. 1, pp. 77–91, 1952.
- [2] M. J. Best and R. R. Grauer, "On the sensitivity of mean-variance-efficient portfolios to changes in asset means: some analytical and computational results," *The review of financial studies*, vol. 4, no. 2, pp. 315–342, 1991.

- [3] R. O. Michaud, "The markowitz optimization enigma: Is 'optimized' optimal?" *Financial analysts journal*, vol. 45, no. 1, pp. 31–42, 1989.
- [4] F. Black and R. Litterman, "Global portfolio optimization," *Financial analysts journal*, vol. 48, no. 5, pp. 28–43, 1992.
- [5] S. Satchell and A. Scowcroft, "A demystification of the black-litterman model: Managing quantitative and traditional portfolio construction," in *Forecasting expected returns in the financial markets*. Elsevier, 2007, pp. 39–53.
- [6] G. He and R. Litterman, "The intuition behind black-litterman model portfolios," *Available at SSRN 334304*, 2002.
- [7] T. Idzorek, "A step-by-step guide to the black-litterman model: Incorporating user-specified confidence levels," in *Forecasting expected returns in the financial markets*. Elsevier, 2007, pp. 17–38.
- [8] W. Bessler and D. Wolff, "A theoretical and empirical analysis of the black-litterman model," in *Algorithms from and for Nature and Life: Classification and Data Analysis*. Springer, 2013, pp. 377–386.
- [9] S. L. Beach and A. G. Orlov, "An application of the black-litterman model with egarch-m-derived views for international portfolio management," *Financial Markets and Portfolio Management*, vol. 21, pp. 147–166, 2007.
- [10] G. Palomba, "Multivariate garch models and the black-litterman approach for tracking error constrained portfolios: an empirical analysis," *Global Business and Economics Review*, vol. 10, no. 4, pp. 379–413, 2008.
- [11] A. Duqi, L. Franci, and G. Torluccio, "The black-litterman model: the definition of views based on volatility forecasts," *Applied Financial Economics*, vol. 24, no. 19, pp. 1285–1296, 2014.
- [12] S. Pyo and J. Lee, "Exploiting the low-risk anomaly using machine learning to enhance the black-litterman framework: Evidence from south korea," *Pacific-Basin Finance Journal*, vol. 51, pp. 1–12, 2018.
- [13] M. Kara, A. Ulucan, and K. B. Atici, "A hybrid approach for generating investor views in black-litterman model," *Expert Systems with Applications*, vol. 128, pp. 256–270, 2019.
- [14] N. E. Huang, Z. Shen, S. R. Long, M. C. Wu, H. H. Shih, Q. Zheng, N.-C. Yen, C. C. Tung, and H. H. Liu, "The empirical mode decomposition and the hilbert spectrum for nonlinear and non-stationary time series analysis," *Proceedings of the Royal Society of London. Series A: mathematical, physical and engineering sciences*, vol. 454, no. 1971, pp. 903–995, 1998.
- [15] W. Shu and Q. Gao, "Forecasting stock price based on frequency components by emd and neural networks," *Ieee Access*, vol. 8, pp. 206 388–206 395, 2020.
- [16] Y. Zhang, B. Yan, and M. Aasma, "A novel deep learning framework: Prediction and analysis of financial time series using ceemd and lstm," *Expert systems with applications*, vol. 159, p. 113609, 2020.
- [17] Y. Lin, Y. Yan, J. Xu, Y. Liao, and F. Ma, "Forecasting stock index price using the ceemdan-lstm model," *The North American Journal of Economics and Finance*, vol. 57, p. 101421, 2021.
- [18] H. Rezaei, H. Faaljoui, and G. Mansourfar, "Intelligent asset allocation using predictions of deep frequency decomposition," *Expert Systems with Applications*, vol. 186, p. 115715, 2021.
- [19] R. Barua and A. K. Sharma, "Using fear, greed and machine learning for optimizing global portfolios: A black-litterman approach," *Finance Research Letters*, vol. 58, p. 104515, 2023.
- [20] W. Jiang, "Applications of deep learning in stock market prediction: recent progress," *Expert Systems with Applications*, vol. 184, p. 115537, 2021.
- [21] M. M. Kumbure, C. Lohrmann, P. Luukka, and J. Porras, "Machine learning techniques and data for stock market forecasting: A literature review," *Expert Systems with Applications*, vol. 197, p. 116659, 2022.
- [22] N. Rehman and D. P. Mandic, "Multivariate empirical mode decomposition," *Proceedings of the Royal Society A: Mathematical, Physical and Engineering Sciences*, vol. 466, no. 2117, pp. 1291–1302, 2010.
- [23] C. Deng, Y. Huang, N. Hasan, and Y. Bao, "Multi-step-ahead stock price index forecasting using long short-term memory model with multivariate empirical mode decomposition," *Information Sciences*, vol. 607, pp. 297–321, 2022.
- [24] Y. Zou and K. He, "Forecasting crude oil risk using a multivariate multiscale convolutional neural network model," *Mathematics*, vol. 10, no. 14, p. 2413, 2022.
- [25] J. Bai, J. Guo, B. Sun, Y. Guo, Q. Bao, and X. Xiao, "Intelligent forecasting model of stock price using neighborhood rough set and multivariate empirical mode decomposition," *Engineering Applications of Artificial Intelligence*, vol. 122, p. 106106, 2023.
- [26] Y. Yao, Z.-y. Zhang, and Y. Zhao, "Stock index forecasting based on multivariate empirical mode decomposition and temporal convolutional networks," *Applied Soft Computing*, vol. 142, p. 110356, 2023.
- [27] X. Lang, Q. Zheng, Z. Zhang, S. Lu, L. Xie, A. Horch, and H. Su, "Fast multivariate empirical mode decomposition," *IEEE Access*, vol. 6, pp. 65 521–65 538, 2018.
- [28] N. Mourad, "Multivariate group-sparse mode decomposition," *Digital Signal Processing*, vol. 137, p. 104024, 2023.
- [29] X. Cai, D. Li, J. Zhang, and Z. Wu, "Ma-emd: Aligned empirical decomposition for multivariate time-series forecasting," *Expert Systems with Applications*, vol. 267, p. 126080, 2025.
- [30] F. Black, "Noise," *The journal of finance*, vol. 41, no. 3, pp. 528–543, 1986.
- [31] R. M. Alrumaih and M. A. Al-Fawzan, "Time series forecasting using wavelet denoising an application to saudi stock index," *Journal of King Saud University-Engineering Sciences*, vol. 14, no. 2, pp. 221–233, 2002.
- [32] H. Hassani, A. Dionisio, and M. Ghodsi, "The effect of noise reduction in measuring the linear and nonlinear dependency of financial markets," *Nonlinear Analysis: Real World Applications*, vol. 11, no. 1, pp. 492–502, 2010.
- [33] W. Bao, J. Yue, and Y. Rao, "A deep learning framework for financial time series using stacked autoencoders and long-short term memory," *PLoS one*, vol. 12, no. 7, p. e0180944, 2017.
- [34] H. Yu, L. J. Ming, R. Sumei, and Z. Shuping, "A hybrid model for financial time series forecasting—integration of ewt, arima with the improved abc optimized elm," *IEEE Access*, vol. 8, pp. 84 501–84 518, 2020.
- [35] J. Wang and J. Liu, "Two-stage deep ensemble paradigm based on optimal multi-scale decomposition and multi-factor analysis for stock price prediction," *Cognitive Computation*, vol. 16, no. 1, pp. 243–264, 2024.
- [36] Z. D. Akşehir and E. Kılıç, "A new denoising approach based on mode decomposition applied to the stock market time series: 2le-ceemdan," *PeerJ Computer Science*, vol. 10, p. e1852, 2024.
- [37] D. S. Broomhead and G. P. King, "Extracting qualitative dynamics from experimental data," *Physica D: Nonlinear Phenomena*, vol. 20, no. 2-3, pp. 217–236, 1986.
- [38] S. Lahmiri, "Minute-ahead stock price forecasting based on singular spectrum analysis and support vector regression," *Applied Mathematics and Computation*, vol. 320, pp. 444–451, 2018.
- [39] Q. Tang, T. Fan, R. Shi, J. Huang, and Y. Ma, "Prediction of financial time series using lstm and data denoising methods," 2021.
- [40] C.-H. Wang, J. Yuan, Y. Zeng, and S. Lin, "A deep learning integrated framework for predicting stock index price and fluctuation via singular spectrum analysis and particle swarm optimization," *Applied Intelligence*, vol. 54, no. 2, pp. 1770–1797, 2024.
- [41] D. Lei, "Black-litterman asset allocation model based on principal component analysis (pca) under uncertainty," *Cluster Computing*, vol. 22, pp. 4299–4306, 2019.
- [42] Z. Wu and N. E. Huang, "Ensemble empirical mode decomposition: a noise-assisted data analysis method," *Advances in adaptive data analysis*, vol. 1, no. 01, pp. 1–41, 2009.
- [43] J.-R. Yeh, J.-S. Shieh, and N. E. Huang, "Complementary ensemble empirical mode decomposition: A novel noise enhanced data analysis method," *Advances in adaptive data analysis*, vol. 2, no. 02, pp. 135–156, 2010.
- [44] M. E. Torres, M. A. Colominas, G. Schlotthauer, and P. Flandrin, "A complete ensemble empirical mode decomposition with adaptive noise," in *2011 IEEE international conference on acoustics, speech and signal processing (ICASSP)*. IEEE, 2011, pp. 4144–4147.
- [45] R. Barua and A. K. Sharma, "Dynamic black litterman portfolios with views derived via cnn-bilstm predictions," *Finance Research Letters*, vol. 49, p. 103111, 2022.
- [46] G. Rilling, P. Flandrin, P. Gonçalves, and J. M. Lilly, "Bivariate empirical mode decomposition," *IEEE signal processing letters*, vol. 14, no. 12, pp. 936–939, 2007.
- [47] N. ur Rehman and D. P. Mandic, "Empirical mode decomposition for trivariate signals," *IEEE Transactions on signal processing*, vol. 58, no. 3, pp. 1059–1068, 2009.
- [48] M. R. Thirumalaisamy and P. J. Ansell, "Fast and adaptive empirical mode decomposition for multidimensional, multivariate signals," *IEEE Signal Processing Letters*, vol. 25, no. 10, pp. 1550–1554, 2018.
- [49] X. Cai and D. Li, "M-edem: A mnn-based empirical decomposition ensemble method for improved time series forecasting," *Knowledge-Based Systems*, vol. 283, p. 111157, 2024.

- [50] S. Bai, J. Z. Kolter, and V. Koltun, "An Empirical Evaluation of Generic Convolutional and Recurrent Networks for Sequence Modeling," Apr. 2018.